

A NEW METHOD OF THE POSITIONING AND ANALYSIS OF THE ROUGHNESS DEVIATION IN FIVE-AXIS MILLING OF EXTERNAL CYLINDRICAL GEAR

Michał CHLOST* , Michał GDULA* 

*Department of Manufacturing Techniques and Automation, Faculty of Mechanical Engineering and Aeronautics,
Rzeszow University of Technology, ul. W. Pola 2, Budynek C, Rzeszów, 35-959, Poland

m.chlost@prz.edu.pl, gdulam@prz.edu.pl

received 7 February 2022, revised 5 April 2022, accepted 24 April 2022

Abstract: Five-axis milling is a modern, flexible and constantly developing manufacturing process, which can be used for the machining of external cylindrical gears by means of cylindrical end mills and special disc mills on universal multi-axis machining centres. The article presents a new method of positioning the tip and the axis of the end mill and the disc cutter in order to ensure a constant value of deviation of the theoretical roughness R_{th} along the entire length of the tooth profile. The first part presents a mathematical model of the five-axis milling process of the cylindrical gear and an algorithm for calculating the R_{th} deviation values. The next section describes the positioning of the end mill and the disc cutter. Then, a new method for the empirical determination of the distribution of the involute root angle Δu_i and the data description by means of the interpolation function are presented and described. In the conducted numerical tests, the influence of the geometrical parameters of the cylindrical gear on the deviation R_{th} is determined, assuming a constant R_{th} value in the five-axis milling process.

Key words: gears, five-axis milling, theoretical roughness, tooth profile error

1. INTRODUCTION

The five-axis milling technology is currently widely used in the manufacture of components with complex geometries, including, among others, the gear wheels. The ability to control the tool in three linear and two rotary axes enables any positioning of the tool in the working space of the machine tool. The flexibility of this machining process allows replacement of the machining carried out with traditional methods, such as hobbing, shaping the surface in a five-axis milling process by means of end mill cutters [1, 2], or the increasingly used disc cutters [3].

In the process of shaping gears, the surface quality and integrity after machining are of great importance. The tooth surface profile is ultimately obtained by applying the finishing methods that were characterised by Karpuschewski et al. [4]. Krömer [5] described the deviation of the tooth shape resulting from the hobbing machining process, considering the tooth line and the tooth profile. Klocke and Staudt [6, 7] presented possible methods of path distribution on the gear tooth flank and analysed the strategy of constant radial distribution of paths, when using the ball nose cutter. Moreover, they investigated the deviation distribution for fixed and variable tool positioning. Staudt and Exner [8] conducted research on the integrity of the tooth flank surface during milling along the tooth line. The machining process was carried out under soft and hardened conditions. Guo et al. [9] conducted research to determine the influence of the geometric parameters of a gear on the distribution of shape deviation. The strategy of constant increase in the involute root angle Δu_i described by Klocke was applied. He also presented a method for determining the position of the end mill cutter, wherein the contact of the cutter operation

surface with the flank surface of the shaped tooth was locally linear.

In addition to the use of end mills and/or ball nose cutter, disc cutters are increasingly used in five-axis machining of gear teeth [3, 10 - 13]. The main advantage of using this type of tool geometry is much easier access of the cutting edge to the lower parts of the inter-tooth notch, possibility of using higher radial in feed values and the associated increase in machining efficiency, as well as the low susceptibility of the tool to elastic deformation.

The description of milling of the cylindrical gears using the disc milling cutter was provided by Talar et al. [13, 14]. They presented the possibility of modification of the profile and line of the gear tooth due to the elastic deformation of the tool.

A more common form of use of the disc milling cutter is the five-axis machining of bevel gears. Deng [10] and Shih [12] presented the method of positioning the disc cutter when machining a free surface, which is the tooth flank of a bevel gear with a circular arc tooth line. Moreover, Shih and Chen [11] presented a method of positioning a disc grinding wheel, with a similar geometry as a disc milling cutter, in the finish machining of a gear with oblique teeth. By appropriately modifying the position of the grinding wheel, they corrected the errors that occurred during the grinding process.

A completely different kinematic solution for machining was investigated by Özel [15], as he analysed the geometric errors of the tooth profile after machining with an end mill cutter. Moreover, he determined the influence of linear interpolation of the tool path on the execution accuracy of the tooth profile.

In the case of finish machining, the elastic deformation of the tool has a significant impact on the accuracy of the machined surface. Solf [16] investigated the issue of the radial correction of

tool deflection during the machining of tothing in the hardened state.

The geometric structure of the flank tooth surface after finish machining and the method of its measurement are equally important. This issue was extensively described by Suh [17], who used the coordinate measurement technique on coordinate measuring machines (CMMs), and by Chmielik et al. [18], where a profilometer was used.

The article proposes and describes a new method of tool positioning in the five-axis machining of a cylindrical gear with a straight tooth line, using the Δu_i distribution function in the mathematical modelling, which allows obtaining a constant deviation of the theoretical surface roughness R_{th} , along the entire tooth profile.

2. MATHEMATICAL MODEL OF THE TOOTH FLANK SURFACE

As Guo et al. [9] described, gear machining on five-axis machine tools consists in positioning the tool and the part in relation to the machine's coordinate system $S_m(x_m, y_m, z_m)$ with origin O_m . The machining system adopted in the five-axis milling of the cylindrical gear with a straight tooth line by means of an end mill cutter for machining is shown in Fig. 1.

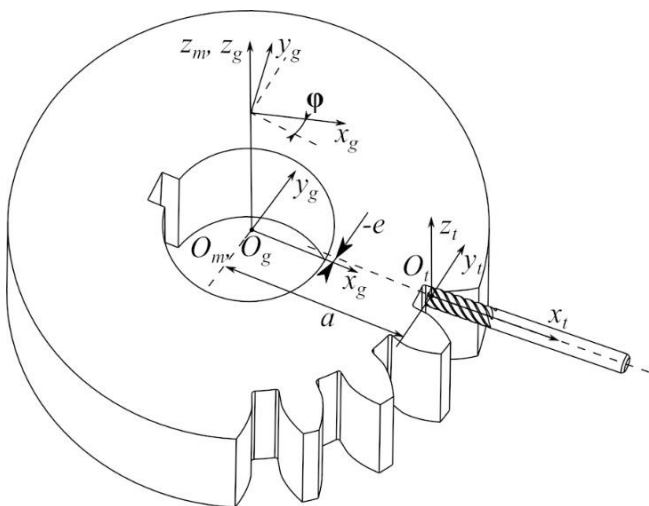


Fig. 1. The machining system adopted in the five-axis milling of the cylindrical gear with straight tooth line

Coordinate systems $S_g(x_g, y_g, z_g)$ with origin O_g and $S_t(x_t, y_t, z_t)$ with origin O_t are assigned to the part and the tool, respectively. The parameters a and e correspond to the positions of the tool tip in the S_m arrangement along the x_m, y_m axes. During machining, the tool makes the main movement along the z_m axis. For each tool, a position defined by the parameters a and e and the tool inclination angle φ are defined, which provides tangential guidance of the cutter action surface to the tooth flank surface, and positioning is achieved by changing the rotary table setting. Depending on the machined side of the tooth, this angle can be positive or negative.

The assumptions for the mathematical model are specified as average parameter values for their ranges of applicability:

- parameters $m, z > 0$, a range was assumed for m (10–20), z (20–70);

- number of tool paths $N \geq 2$, a range was assumed for N (10–20);
- pressure angle $\alpha > 0$, a range was assumed for α (20°–30°);
- the parameter of the empirical function was determined experimentally and is $x = 1/0.667$;
- diameter d of the cylindrical tool and radius r of the disc tool $d, r > 0$.

The basic geometrical parameters of a gear are shown in Fig. 2 and described by the equations Eqs. (1)–(13), which were described by Burek et al. [1].

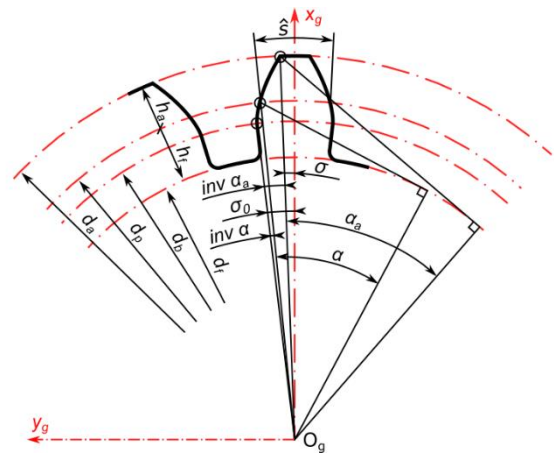


Fig. 2. Basic gear dimensions

Input parameters: m – module, z – number of teeth, α – pressure angle.

$$d_p = m \cdot z \quad (1)$$

$$h_a = m \quad (2)$$

$$h_f = 1.25 \cdot m \quad (3)$$

$$d_a = d_p + 2 \cdot h_a \quad (4)$$

$$d_f = d_p - 2 \cdot h_f \quad (5)$$

$$d_b = d \cdot \cos(\alpha) \quad (6)$$

$$r_b = \frac{d_b}{2} \quad (7)$$

$$\text{inv } \alpha = \tan(\alpha) - \alpha \quad (8)$$

$$\alpha_a = \cos^{-1} \left(\frac{d_b}{d_a} \right) \quad (9)$$

$$\text{inv } \alpha_a = \tan(\alpha_a) - \alpha_a \quad (10)$$

$$\sigma = \frac{\hat{s}}{d} \cdot \frac{180^\circ}{\pi} \quad (11)$$

$$\sigma_0 = \sigma + \text{inv } \alpha \quad (12)$$

$$u = \alpha_a + \text{inv } \alpha_a \quad (13)$$

where d_p – pitch diameter, h_a – addendum, h_f – dedendum, d_a – addendum diameter, d_f – dedendum diameter, d_b – basic diameter, r_b – basic radius, $\text{inv } \alpha$ – involute function of angle α , α_a – pressure angle on addendum, $\text{inv } \alpha_a$ – involute function of angle α_a , σ – half angle on pitch diameter, σ_0 – half angle on basic diameter and u – root angle.

The flank surface of the tooth can be described using two parameters (u, v) [19], as shown in Fig. 3. The parameter u , which is

the root angle of the involute subjected to subsequent discretisation, describes the tooth outline, and the parameter v describes the tooth line.

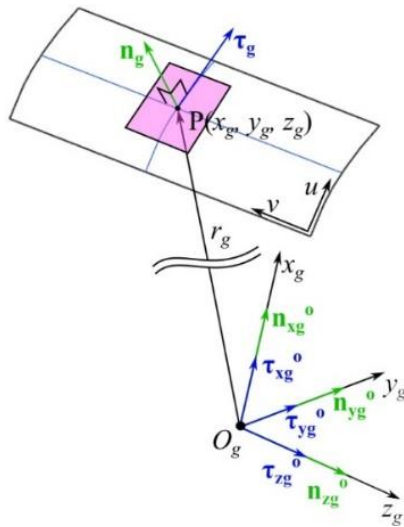


Fig. 3. Parametric description of the tooth flank surface

The position vector r_g and the normal vector n_g of the surface are described by the relationship in Eq. (14):

$$\begin{cases} r_g(u, v) = [x_g & y_g & z_g & 1] \\ n_g(u, v) = [n_{xg} & n_{yg} & n_{zg} & 1] \end{cases} \quad (14)$$

Where (x_g, y_g, z_g) are the coordinates of the end point P of position vector r_g described by Eq. (15), and (n_{xg}, n_{yg}, n_{zg}) are component vectors of the vector n_g normal to the tooth flank surface, described by Eq. (16):

$$\begin{bmatrix} x_g \\ y_g \\ z_g \end{bmatrix} = \begin{bmatrix} r_b \cos(\sigma_0 + u) + r_b u \sin(\sigma_0 + u) \\ r_b \sin(\sigma_0 + u) - r_b u \cos(\sigma_0 + u) \\ pv \end{bmatrix} \quad (15)$$

$$\begin{bmatrix} n_{xg} \\ n_{yg} \\ n_{zg} \end{bmatrix} = \begin{bmatrix} pr_b u \sin(\sigma_0 + u) \\ -pr_b u \cos(\sigma_0 + u) \\ 0 \end{bmatrix} \quad (16)$$

where r_b is the radius of the base circle, and p is a parameter describing the width of the gear rim.

An additional parameter that allows the correct positioning of the tool axis is the tangent vector τ_g to the surface at point $P(x_g, y_g, z_g)$, which is described by the dependencies Eqs. (17) and (18):

$$\tau_g(u, v) = [\tau_{xg} \quad \tau_{yg} \quad \tau_{zg} \quad 1] \quad (17)$$

where

$$\begin{bmatrix} \tau_{xg} \\ \tau_{yg} \\ \tau_{zg} \end{bmatrix} = \begin{bmatrix} r_b u \cos(\sigma_0 + u) \\ r_b u \sin(\sigma_0 + u) \\ 0 \end{bmatrix} \quad (18)$$

The transformation of the part system S_g to the machine coordinate system S_m is carried out through the rotation matrix M_{mg} , determined by the relation Eq. (19):

$$M_{mg} = \begin{bmatrix} \cos \varphi & -\sin \varphi & 0 & 0 \\ \sin \varphi & \cos \varphi & 0 & 0 \\ 0 & 0 & 1 & -p \\ 0 & 0 & 0 & 1 \end{bmatrix} \quad (19)$$

where φ is the angle of the machine part's rotation on the machine tool turntable.

The same should be done with the tool coordinate system S_t , whose transformation to the machine system S_m takes the form of the translation matrix M_{mt} , determined by the relation Eq. (20):

$$M_{mg} = \begin{bmatrix} 1 & 0 & 0 & a \\ 0 & 1 & 0 & e \\ 0 & 0 & 1 & 0 \\ 0 & 0 & 0 & 1 \end{bmatrix} \quad (20)$$

where the parameters a and e define the position of the tool in relation to the x_m and y_m axes.

3. CALCULATION OF R_{th} DEVIATION

The geometric relationships that allow the determination of the R_{th} deviation of the theoretical surface roughness and the geometric system of the five-axis machining adopted for the study are shown in Fig. 4.

In order to calculate the R_{th} deviation, it is necessary to determine the distance CD. Points A(x_{gA}, y_{gA}) and B(x_{gB}, y_{gB}) are the points that describe the flank surface of the tooth, where point A represents the first position of the tool, and point B represents the next position of the tool. Point C is at the point of intersection of the line segments AC and BC that are tangential to the tooth profile at points A and B, respectively. Segments AC and BC represent a group of lines described by the linear relationship in Eq. (21), where the parameters k_A and k_B described by the relationship Eq. (22) determine their slopes in relation to the x_g axis:

$$\begin{cases} x_{gA} = k_A y_{gA} + b_A \\ x_{gB} = k_B y_{gB} + b_B \end{cases} \quad (21)$$

where

$$\begin{cases} k_A = -\frac{n_{gyA}}{n_{gxA}} \\ k_B = -\frac{n_{gyB}}{n_{gxB}} \end{cases} \quad (22)$$

After determining the slopes of the lines, it becomes possible to derive Eq. (23) describing the term b of the linear equation of lines:

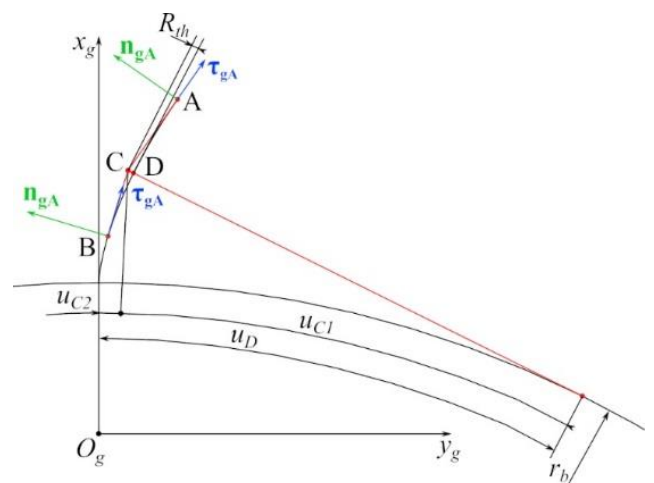


Fig. 4. The geometric structure allowing determination of the R_{th} deviation

$$\begin{cases} b_A = x_{gA} - (k_A y_A) \\ b_B = x_{gB} - (k_B y_B) \end{cases} \quad (23)$$

This allowed the creation of the system of equations Eq. (24) necessary to determine the coordinates of the intersection point C(x_{gC} , y_{gC}):

$$\begin{cases} x_{gC} = k_B \frac{b_A - b_B}{k_B - k_A} + b_B \\ y_{gC} = \frac{b_A - b_B}{k_B - k_A} \end{cases} \quad (24)$$

In order to determine the coordinates of the point D(x_{gD} , y_{gD}), the values of the involute root angle u_D should be determined. The determination of the u_D angle is described by the relationships Eqs. (25)–(28):

$$u_D = u_{C1} + u_{C2} \quad (25)$$

where

$$u_{C1} = \tan^{-1} \left(\frac{y_{gC}}{x_{gC}} \right) \quad (26)$$

$$OC = \sqrt{x_{gC}^2 + y_{gC}^2} \quad (27)$$

$$u_{C2} = \cos^{-1} \left(\frac{r_b}{OC} \right) \quad (28)$$

Finally, the coordinates of point D are determined from the system of equations Eq. (29):

$$\begin{bmatrix} x_{gD} \\ y_{gD} \\ z_{gD} \end{bmatrix} = \begin{bmatrix} r_b \cos(\sigma_0 + u_D) + r_b u \sin(\sigma_0 + u_D) \\ r_b \sin(\sigma_0 + u_D) - r_b u \cos(\sigma_0 + u_D) \\ pv \end{bmatrix} \quad (29)$$

4. POSITIONING OF THE TOOL

Three types of tool geometry are used for the five-axis machining of gears, in both soft and hardened conditions. The basic, and—so far—the most frequently used, tools are end mills with ball or cylindrical geometry [1, 6, 7, 8, 15]. Research conducted so far [6, 3] has shown that the machining conditions and machinability in the five-axis flank milling method with an end mill cutter are definitely better than with a ball end mill cutter. This can also be observed in terms of the difference in the geometry of the remains

after machining on the tooth flank surfaces and in the efficiency of machining of the toothing.

A disc cutter is the third and increasingly frequently used tool for machining gears on multi-axis milling computerised numerical control (CNC) machines. The sharp apex angle of the cutting inserts provides much better access of the tool along the entire depth of the inter-tooth notch, making it possible to machine gears with much smaller modules than in the case of an end mill cutter.

The machining system and the five-axis machining model of the tooth flank with an end mill cutter, which works tangentially to point A, are shown in Fig. 5(a). The tool axis is defined at location I as the tangent vector τ_{gA} , expressed as unit vector τ_{gA}° , and at location II as tangent vector τ_{gB} , expressed as unit vector τ_{gB}° . The position of the tool centre point (TCP), which is the zero point of the tool coordinate system S_t , is defined in Eq. (30) as a translation in the normal direction by the product with the unit vector $n_{gA(B)}^\circ$, which is determined by Eq. (31), and half the tool diameter d with reference to the point C, which describes the peak of the R_{th} deviation:

$$\begin{cases} x_{TCP} = x_{gC} + n_{xgA(B)}^\circ \frac{d}{2} \\ y_{TCP} = y_{gC} + n_{ygA(B)}^\circ \frac{d}{2} \\ z_{TCP} = z_{gC} \end{cases} \quad (30)$$

where

$$\begin{cases} n_{xgA(B)}^\circ = \frac{n_{xgA(B)}}{\|n_{xgA(B)}\|} \\ n_{ygA(B)}^\circ = \frac{n_{ygA(B)}}{\|n_{ygA(B)}\|} \\ n_{zgA(B)}^\circ = 0 \end{cases} \quad (31)$$

In this case, the unequivocal position of the tool in the space of a five-axis CNC machine tool can be determined from Eq. (32):

$$[x_{TCP}, y_{TCP}, z_{TCP}, \tau_{xgA(B)}^\circ, \tau_{ygA(B)}^\circ, 0] \quad (32)$$

The machining system and the five-axis machining model presented in Fig. 5(b) refer to the use of the disc milling cutter. Proper positioning of the tool consists in leading the action surface tangential to the tooth profile. As in the case described earlier, transformation of the TCP position described by Eq. (33) should be made, which in the reference position coincides with point C.

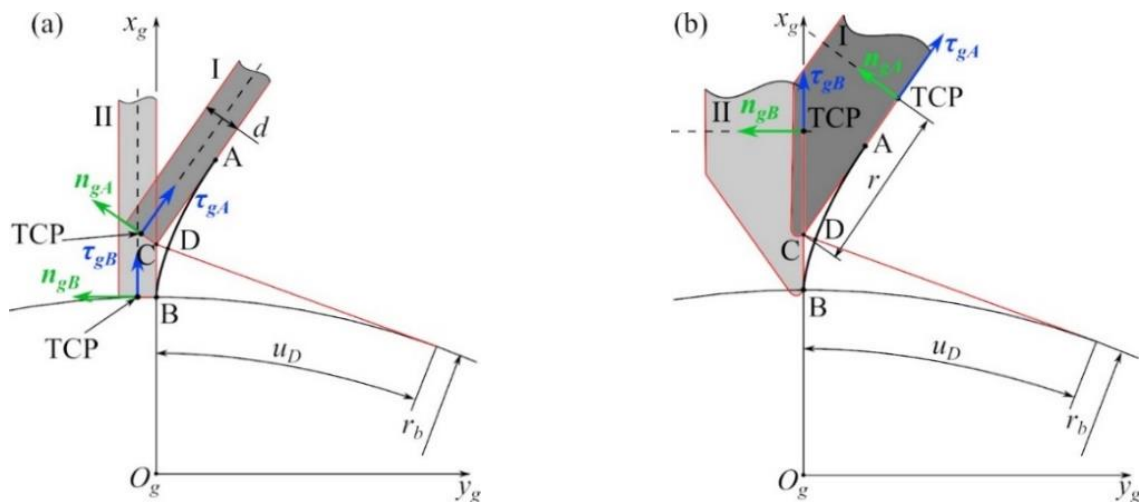


Fig. 5. Machining system and positioning method: (a) for end milling cutter; (b) for disc milling cutter in five-axis machining of toothing
Abbreviation: TCP, tool centre point

In the configuration of the machining system considering position I of the tool as the axis of rotation, the vector \mathbf{n}_{gA} normal to the curve at point A was adopted, expressed as the unit vector \mathbf{n}_{gA}° , while in position II, the normal vector \mathbf{n}_{gB} to the curve at point B, expressed as the unit vector \mathbf{n}_{gB}° , was adopted.

The translation of the TCP relative to the point C is determined by the product of the unit vector $\boldsymbol{\tau}_{gA(B)}^\circ$, expressed by Eq. (34), and the tool radius r .

$$\begin{cases} x_{TCP} = x_{gC} + \boldsymbol{\tau}_{xgA(B)}^\circ r \\ y_{TCP} = y_{gC} + \boldsymbol{\tau}_{ygA(B)}^\circ r \\ z_{TCP} = z_{gC} \end{cases} \quad (33)$$

where

$$\begin{cases} \boldsymbol{\tau}_{xgA(B)}^\circ = \frac{\boldsymbol{\tau}_{xgA(B)}}{\|\boldsymbol{\tau}_{xgA(B)}\|} \\ \boldsymbol{\tau}_{ygA(B)}^\circ = \frac{\boldsymbol{\tau}_{ygA(B)}}{\|\boldsymbol{\tau}_{ygA(B)}\|} \\ \boldsymbol{\tau}_{zgA(B)}^\circ = 0 \end{cases} \quad (34)$$

In turn, in this case, the unequivocal position of the tool in the space of a five-axis CNC machine tool can be determined from Eq. (35).

$$[x_{TCP}, y_{TCP}, z_{TCP}, \boldsymbol{n}_{xgA(B)}^\circ, \boldsymbol{n}_{ygA(B)}^\circ, 0] \quad (35)$$

The above method of positioning the disc milling cutter can find an analogous application in the case of a disc grinding wheel in the grinding of gear teeth on multi-axis CNC milling machines. The advantage of this solution is the possibility of milling and grinding the gears without the need to attach the part in another machine tool. This results in an increase in the dimensional and shape accuracy of the gear wheel. This is of particular importance in the aspect of manufacturing of aircraft gears, as well as special purpose gears for the defence industry.

5. FIVE-AXIS MILLING STRATEGIES FOR TOOTHING

The value of the theoretical surface roughness deviation R_{th} and the machining time T_c depend on the adopted positioning strategy of the milling cutter. In the literature, three basic cases of tool positioning have been distinguished [5, 6, 7, 9] for which a collate was made, assigning a given strategy to the R_{th} deviation of a gear tooth profile. These collates are presented in Fig. 6. Fig. 6(a) shows the distribution of the R_{th} deviation resulting from the arrangement of the tool paths along the tooth profile, according to the strategy of maintaining a constant increase in the involute root angle Δu_i . It was noticed that the maximum deviation R_{th} occurs in the upper part of the tooth and is 0.007 mm, and the smallest at the tooth foot, where its value is 0.0002 mm. In the case of the collate in Fig. 6(b), the distribution of paths is implemented as a strategy of constant division of the tooth height in the radial direction. In this case, the greatest deviation occurs in the lower part of the tooth and is 0.016 mm, while the smallest deviation occurs at the upper part of the tooth and is 0.0018 mm.

The last collate shown in Fig. 6(c) illustrates the strategy according to which the tool paths are distributed in such a way that the R_{th} deviation is constant along the entire length of the tooth profile. The deviation in this case is 0.0032 mm.

Depending on the adopted positioning strategy of the tool, a variable distribution of the value of the R_{th} deviation can be observed, which depends on the adopted function describing the

change of the involute root angle u . All the above figures show the distribution of the R_{th} deviation according to the machining strategy (tool positioning) for a tooth with the same geometric parameters and the same adopted number of paths. On this basis, it should be concluded that for the same number N of paths, the third strategy provides the smallest mean R_{th} deviation in the distribution along the entire tooth profile.

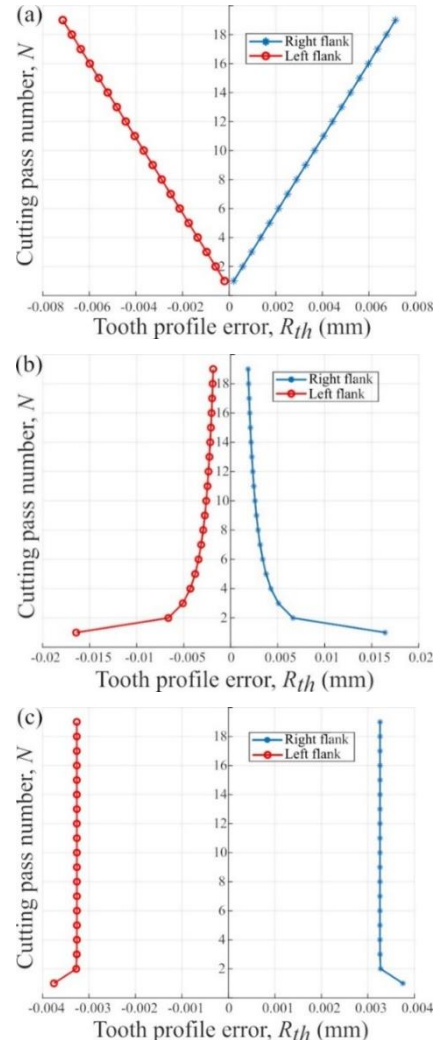


Fig. 6. Machining strategies in relation to the R_{th} deviation of the tooth profile: (a) strategy of constant increment of the involute root angle u ; (b) strategy of constant radial distribution of toolpaths; (c) strategy of constant deviation R_{th}

6. EMPIRICAL DETERMINATION OF THE DISTRIBUTION OF THE INVOLUTE ROOT ANGLE u

In order to define the function describing the R_{th} deviation distribution, it was necessary to use an empirical model. Using the computer-aided design (CAD) software, we developed a parametric sketch showing the tooth profile [1, 20] and the individual tangent lines that define the vertices of the R_{th} deviation, as shown in Fig. 7.

With the help of geometric constraints, a constant distance of the vertices from the tooth profile was imposed, and lines denoting the unwind angle of the involute were drawn. Then, based on the geometry analysis tool in the CAD environment, the values of the

unwind angle Δu_i for the individual tool paths were read. The tolerance value of the researched CAD model was set at 0.0001 mm. Based on the measured values, a graph of the value of the unwind angle Δu_i was developed, which is assumed for a given tool path i . This function is described by the relationship in Eq. (36).

$$\Delta u_i = \sqrt[x]{\frac{u^{xi}}{N-1}} \quad (36)$$

where u – involute root angle, N – number of considered tool-paths, $i=(0, 1, 2, \dots(N-1))$ – consecutive toolpaths.

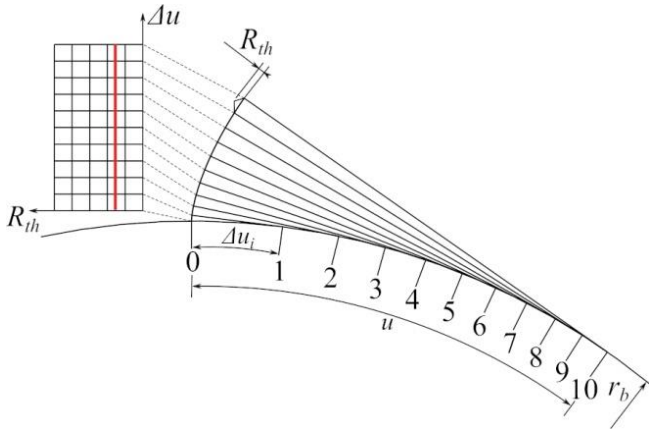


Fig. 7. Distribution of Δu_i for the constant R_{th} deviation strategy

In order to determine the degree of the root from Eq. (36), a series of x values ranging from 1/0.6 to 1/0.7 with a step size of 0.001 were analysed by the iterative method.

As a result of the simulation, the root base equal to 1/0.667 was selected since, for this value, the smallest deviation from the base function was observed for Eq. (36). The superimposed graphs of the empirically determined points and the function described by Eq. (36) with the base $x=1/0.667$ are shown in Fig. 8.

7. ANALYSIS OF R_{th} DEVIATION

For the adopted strategy of constant R_{th} deviation, numerical tests were carried out for both the end milling and the disc milling cutters. The results of these tests are shown in Fig. 9.

In individual cases, the change in the R_{th} deviation was considered depending on the number of passes of the tool N , the number of gear teeth z , the change in the normal tooth modulus m_n and the variable value of the pressure angle α , respectively shown in Fig. 9.

It was found that the results of the simulation of machining along the tooth line for both tool geometries were comparable. By analysing the results of the simulation tests, it can be concluded that the greatest increase in the value of the R_{th} deviation occurs when the number of tool passes changes as shown in Fig. 9(a), where the smallest R_{th} deviation value was 0.0029 mm for the number of paths $N = 20$; for the number of paths $N = 10$, the R_{th} deviation was 0.0118 mm.

The smallest differences in the values of the R_{th} deviation were observed for the variable value of the number of teeth of the gear as shown in Fig. 9(b), where for the number of teeth $z = 20$,

the R_{th} deviation is 0.0029 mm, while for the number of teeth $z = 70$, the highest R_{th} deviation value of 0.0040 mm was noted.

In the case of different values of the modulus m_n and the pressure angle α being defined as shown in Fig. 9(c) and (d), respectively, an increase of the R_{th} deviation is comparable. When changing the value of the module for $m_n = 10$ mm, the value of the R_{th} deviation was the smallest and amounted to 0.0029 mm, and for the value of $m_n = 20$, the value of the R_{th} deviation was 0.0058 mm. Similarly, in the case of the pressure angle α , the smallest R_{th} deviation value was noted for $\alpha = 20^\circ$ and was the same as in the case of the set module value $m_n = 10$ mm, while the largest R_{th} deviation value equal to 0.0057 mm was noted for the angle $\alpha = 30^\circ$.

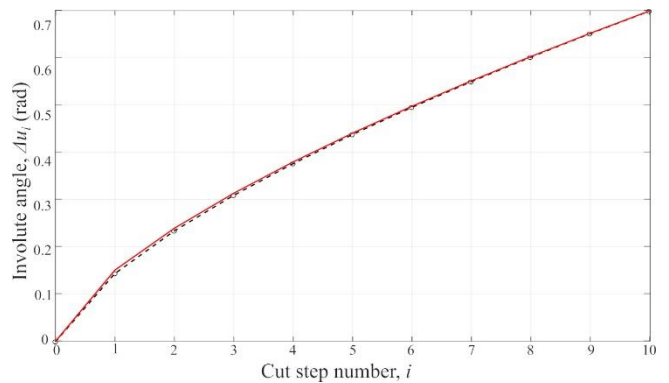


Fig. 8. Approximation of values determined empirically by the function describing the distribution of the involute root angle Δu

Moreover, it was observed, that with an increase in the value of individual parameters of both the gear wheel and the machining process, the value of the R_{th} deviation also increases, wherein depending on the parameter, this change has a different characteristic and tendency.

Another phenomenon observed is the increased value of the R_{th} deviation for the first tool path. This deviation is caused by a poorer fit of the approximation function for small involute root angles Δu_i , which occur in the tooth flank's bottom area, but these regions do not participate directly in the transmission of torque due to the apical clearance.

8. SUMMARY

The article presents and describes a new method of tool positioning assuming a constant R_{th} deviation in the five-axis machining of gears on universal CNC machines. A new mathematical model has been presented that allows determining the value of the R_{th} deviation and the position of the tool during the five-axis machining depending on the tool geometry.

As a result of the numerical tests and numerous simulations, the relationship between the gear wheel parameters and the R_{th} deviation is determined. The number of tool paths N has the greatest impact on the amount of the R_{th} deviation, while the number of teeth in the gear wheel has the smallest impact. The parameters such as the modulus m_n and the pressure angle α have a comparable coefficient of influence on the increase of the R_{th} deviation.

The adopted methodology and the developed assumptions of the five-axis machining strategy are a new proposal to solve the problem of the uneven distribution of the R_{th} deviation in the hobbing process. Depending on the expected results of further research carried out by the authors of this work, it is possible to use another function describing the distribution of the involute root

angle u , which will significantly increase the possibilities of shaping the flank profiles of the teeth. Another advantage is an increase of the machining effectiveness of gear wheels, by obtaining a much smaller R_{th} deviation than in the case of the strategy of constant increase of the involute root angle u .

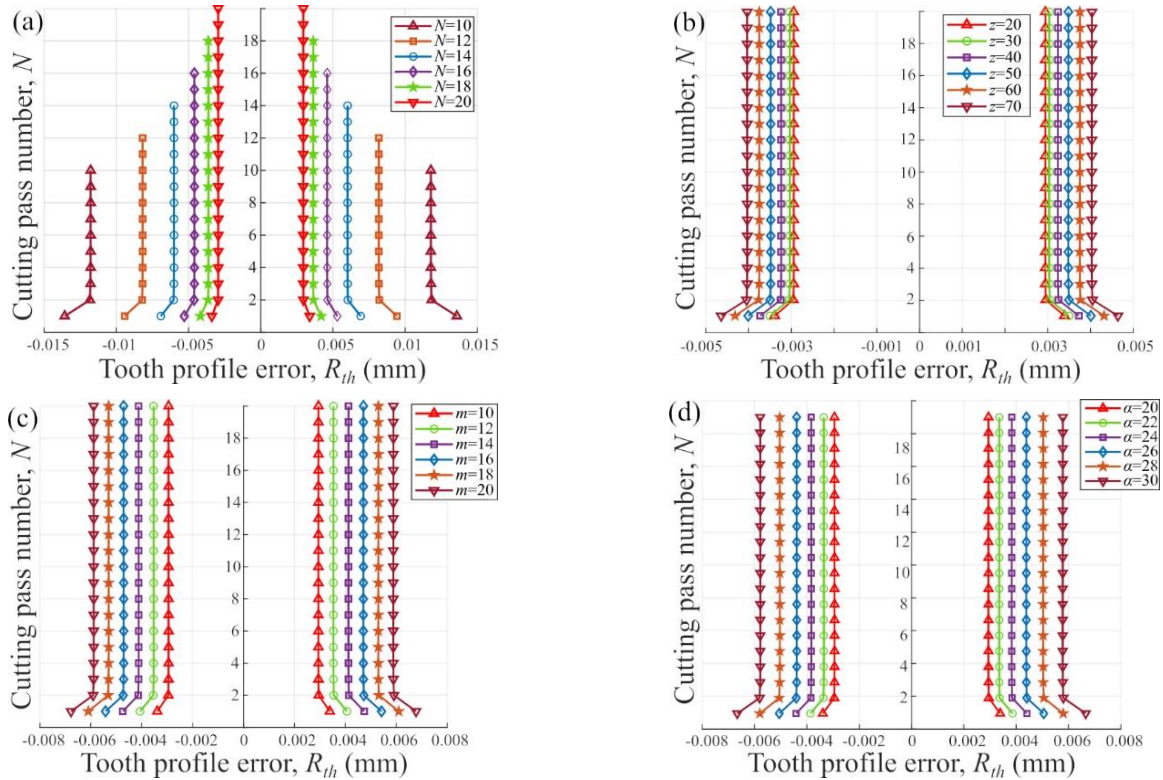




Fig. 9. Influence of the gear wheel parameters and the machining on the R_{th} deviation : (a) number of paths N ; (b) number of teeth z ; (c) normal modulus m_n ; (d) angle of pressure α

REFERENCES

- Burek J, Gdula M, Plodzień M, Buk J. Gear's tooth profile shaping in dialog and parametric programming. *Mechanik*. 2015 Feb;2:142/7.
- Safarov DT, Kondrashov AG, Khafizov II. Improving the process efficiency of helical gears' toothed rims at the stage of pre-production. *IOP Conference Series: Materials Science and Engineering*. 2019;570(012024).
- Gaiser U. 5-Axis Gear Manufacturing Gets Practical. *Gear Technology*. 2017;(March/April):32-4.
- Karpuschewski B, Knoche HJ, Hipke M. Gear finishing by abrasive processes. *CIRP Annals - Manufacturing Technology*. 2008;57(2): 621-40.
- Krömer M, Sari D, Löpenhaus C, Brecher C. Surface Characteristics of Hobbed Gears. *Gear Technology [Internet]*. 2017 [cited 2020 Feb 4];(July):68-75. www.geartechnology.com
- Klocke F, Brumm M, Staudt J. Quality and surface of gears manufactured by free form milling with standard tools. *Gear Technology*. 2015;(January/February):64-9.
- Staudt J, Löpenhaus C, Klocke F. Performance of Gears Manufactured by 5-Axis Milling. *Gear Technology [Internet]*. 2017:58-65. www.geartechnology.com
- Staudt J, Exner P. Einfluss der Oberflächenstruktur beim 5-Achs-Fräsen von Verzahnungen auf das Einsatzverhalten [Internet]. 2017 [cited 2020 Jan 24]. www.fva-net.de
- Guo E, Ren N, Liu Z, Zheng X, Zhou C. Study on tooth profile error of cylindrical gears manufactured by flexible free-form milling. *International Journal of Advanced Manufacturing Technology*. 2019;103(9-12):4443-51.
- Deng XZ, Li GG, Wei BY, Deng J. Face-milling spiral bevel gear tooth surfaces by application of 5-axis CNC machine tool. *International Journal of Advanced Manufacturing Technology*. 2014;71(5-8):1049-57.
- Shih YP, Chen SD. A flank correction methodology for a five-axis CNC gear profile grinding machine. *Mechanism and Machine Theory [Internet]*. 2012;47(1):31-45. <http://dx.doi.org/10.1016/j.mechmachtheory.2011.08.009>
- Shih YP, Sun ZH, Wu FC. A disk tool cutting method for bevel gear manufacture on a five-axis machine. *International Journal of Advanced Manufacturing Technology*. 2018;94(1-4):855-65.
- Talar R, Jablonski P, Ptaszynski W. New method of machining teeth on unspecialised machine tools. *Tehnicki Vjesnik*. 2018 Feb 1;25(1):80-7.
- Talar R, Jablonski P. Modelling of spur gear cutting kinematics for multipurpose milling center. In: 2016 21st International Conference on Methods and Models in Automation and Robotics. Institute of Electrical and Electronics Engineers Inc.; 2016. p. 1133-6.
- Özel C. A study on cutting errors in the tooth profiles of the spur gears manufactured in CNC milling machine. *International Journal of Advanced Manufacturing Technology*. 2012;59(1-4):243-51.

16. Solf M, Bieker R, Löpenhaus C, Klocke F, Bergs T. Influence of the machining strategy on the resulting properties of five-axis hard-milled bevel gears. Proceedings of the Institution of Mechanical Engineers, Part C: Journal of Mechanical Engineering Science. 2019;233(21–22):7358–67.
17. Suh SH, Lee ES, Kim HC, Cho JH. Geometric error measurement of spiral bevel gears using a virtual gear model for STEP-NC. International Journal of Machine Tools and Manufacture. 2002 Feb;42(3):335–42.
18. Chmielik IP, Czarniecki H. Evaluation of gear tooth 3D surface topography. Mechanik. 2015 Jul;7:101–10.
19. Litvin FL, Fuentes A. Gear Geometry and Applied Theory. Gear Geometry and Applied Theory. Cambridge University Press; 2004.
20. Twardoch K. Digital Geometric Modelling of Teeth Profile By Using Cad Methodology. Scientific Journal of Silesian University of Technology Series Transport. 2014;82:271–9.

Michał Chlost:  <https://orcid.org/0000-0001-9420-4239>

Michał Gdula:  <https://orcid.org/0000-0001-7760-4986>